

Electronic Supplementary Information for

Hierarchical Porous TiO₂@C Hollow Microspheres: One-pot Synthesis and Enhanced Visible-Light Photocatalysis

Jiandong Zhuang,^{a,b} Qinfen Tian,^b Hu Zhou,^a Qian Liu,^{,a} Ping Liu^b and Hongmei Zhong^a*

*^aThe State Key Lab of High Performance Ceramics and Superfine Microstructure, Shanghai
Institute of Ceramics, Chinese Academy of Sciences, Shanghai 200050, China*

*^bFujian Provincial Key Laboratory of Photocatalysis--State Key Laboratory Breeding Base,
Fuzhou University, Fuzhou 350002, China*

Supporting Information 1

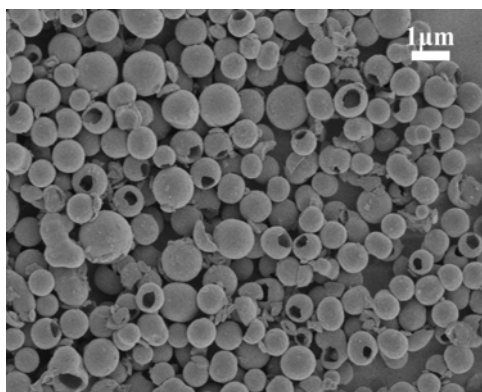


Fig. S1 SEM image of the TiO₂ hollow sphere.

The morphology of TiO₂ hollow microspheres (THMs), which obtained by an extra calcination of TCHMs at 500 °C, is shown in Figure S1. It can be observed in the image that the hollow structure is still retained after the removal of carbon component by calcination treatment.

* To whom correspondence should be addressed. E-mail: qianliu@sunm.shcnc.ac.cn; Phone: +86-(0)21-52412612.

Supporting Information 2

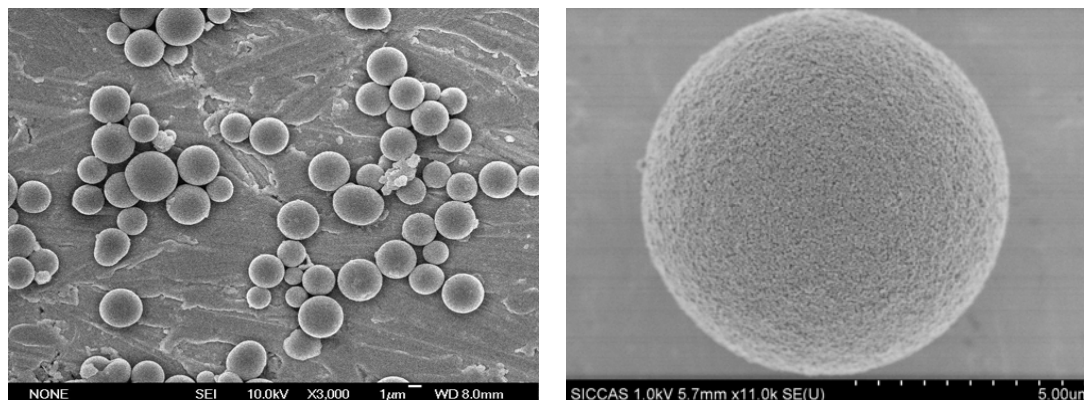


Fig. S2 SEM image of the as-synthesized TCMs sample.

The morphology of porous $\text{TiO}_2@\text{C}$ solid microspheres is shown in Fig. S2. The diameter of spherically shaped particles is not uniform (in a range of 1-6 μm) and much larger than that of the TCHMs particles.

Supporting Information 3

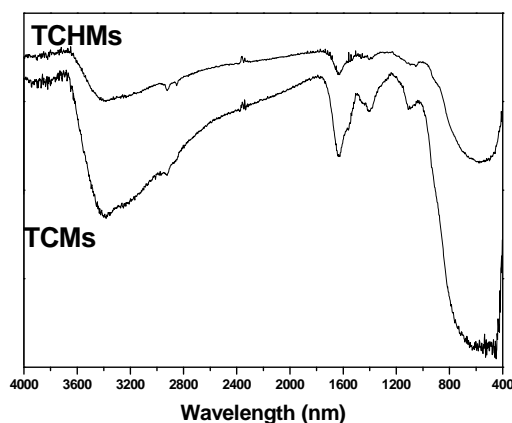


Fig. S3 FTIR spectrum for hybrid inorganic-organic nanocomposites TCHMs and TCMs

FTIR spectra were recorded on a Thermo Nicolet FT-IR NEXUS 670 spectrometer. As shown in Fig. S3, the band at 3400 cm^{-1} is a consequence of associated $-\text{OH}$ groups stretch vibrations of the adsorbed water. Stretching vibrations in the region of $3000\text{-}2800\text{ cm}^{-1}$ and deformation vibrations in the region of $1470\text{-}1350\text{ cm}^{-1}$ are

related to aliphatic structures in the investigated products. The band at around ~ 1700 cm^{-1} is related to the stretching of C=O in linear aliphatic aldehydes or ketones and carboxyls formed in an oxygen atmosphere. The band in the region $1020\sim 1140$ cm^{-1} can be attributed to C-O single bonds. The peaks intensity decreases as a result of the decreasing carbon amount of TCHMs. Moreover, compared with the spectrum of TCMs, no new band on the spectrum of TCHMs can be observed, indicating the DDA was totally removed with ethanol by five cycles.

Supporting Information 4

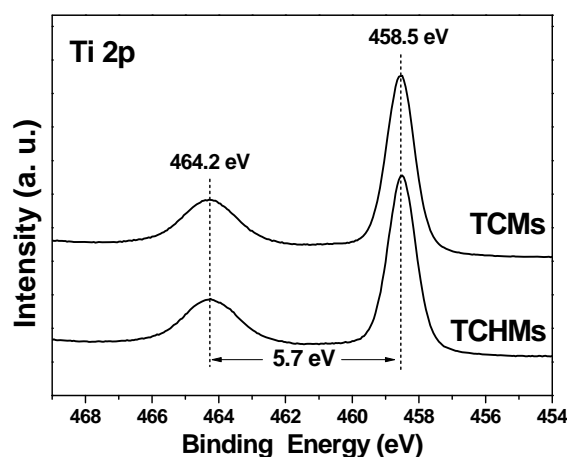


Fig. S4 Ti 2p spectra of the as-synthesized hybrid TiO_2 -C composites.

X-ray photoelectron spectroscopy (XPS) analysis was conducted on an ESCALAB 250 photoelectron spectroscopy (Thermo Fisher Scientific) using Al $K\alpha$ X-ray beam (1486.6 eV). The XPS peaks of Ti $2p_{3/2}$ and $2p_{1/2}$ are located at about 458.5 eV and 464.2 eV with a good symmetry, indicating that the chemical valence of Ti is +4 and in octahedral coordination with oxygen. Moreover, the chemical environments for Ti and O_L are not changed, strongly suggesting that carbon and nitrogen do not enter the TiO_2 crystal lattice under the mild solvothermal conditions.

Supporting Information 5

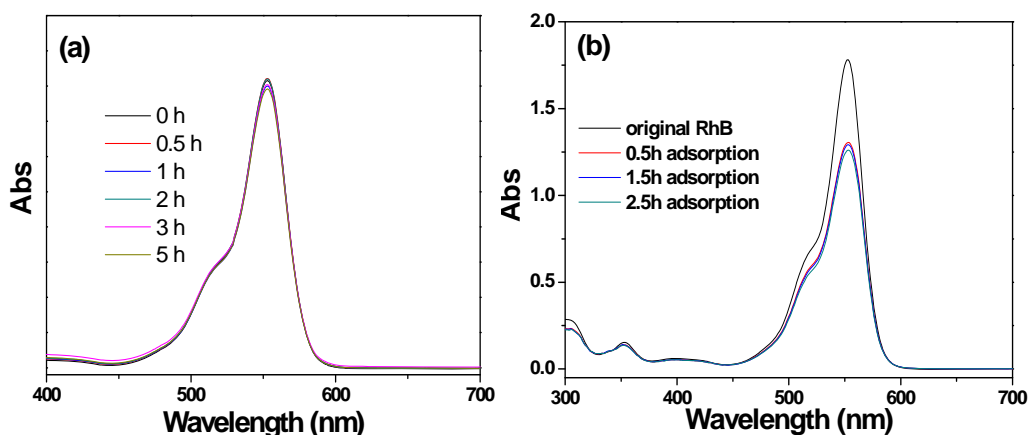


Fig. S5 Temporal UV-vis adsorption spectral changes for the RhB solution (20 μM) as a function of (a) visible light irradiation time (without photocatalyst), and (b) adsorption time over sample TCHMs in the dark.

As observed in Fig. S5, the control experiments were performed under different conditions: (1) with visible light irradiation but in the absence of photocatalysts and (2) in the presence of TCHMs but in the dark. It can be seen in Fig. S5a that RhB has a major absorption band at 554 nm. During irradiation, small changes in both the absorption peak intensity and wavelength shifts are observed with increasing time, indicating that the RhB solution is fairly stable to visible light irradiation. Moreover, as shown in Fig. S5b, the adsorption-desorption equilibrium of RhB over TCHMs can be established within 30 min.

Supporting Information 6

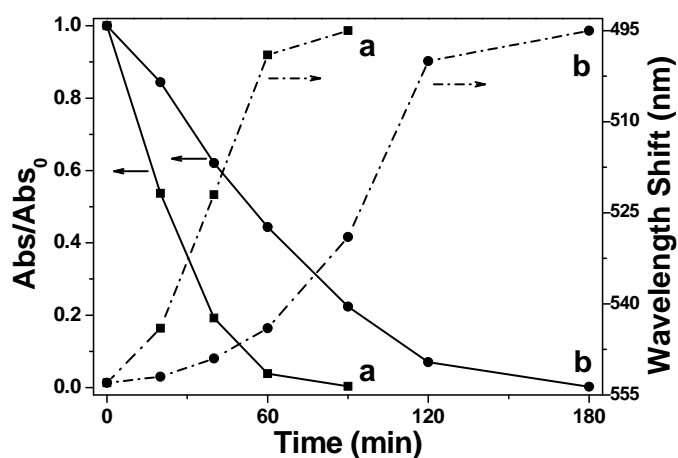


Fig. S6 Absorbance changes at 553 nm (solid curves) and the corresponding wavelength shifts (dash curves) of the spectra of RhB solutions over (a) TCHMs and (b) TCMs as a function of visible light ($450 \leq \lambda \leq 800$ nm) irradiation time.

Fig. S6 summarizes the absorbance changes of the maximum absorbance and the corresponding wavelength shifts of the RhB solution over the visible-light irradiated photocatalysts. In comparison with that of the TCMs, the TCHMs shows higher efficiencies in the visible-light-driven N-deethylation and the photocatalytic degradation of RhB dye.

Supporting Information 7

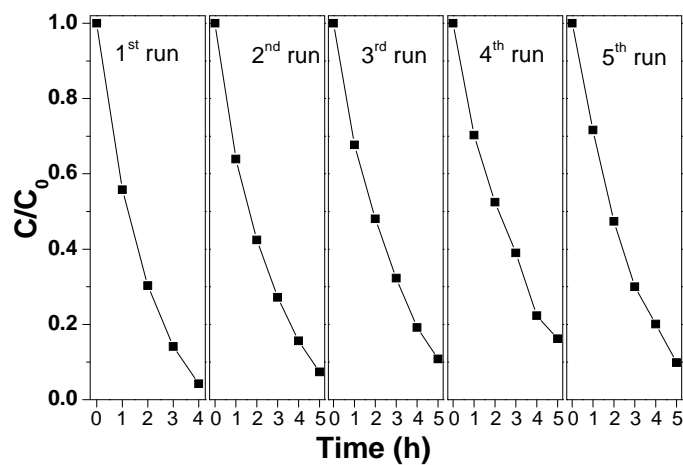


Fig. S7 Recycled photodegradation of RhB under the irradiation of visible light over sample TCHMs. The concentration of RhB is monitored by examining the integrated area of the main RhB absorption peak (400 - 615 nm).

The stability of sample TCHMs was examined for degradation of RhB during a five cycle experiment. Fig. S7 displays the durability of the photocatalytic activity of TCHMs toward the degradation of RhB under visible light irradiation. After five cycles, the photocatalytic activity decreases slightly, which indicates that sample TCHMs exhibits good stability.

Supporting Information 8

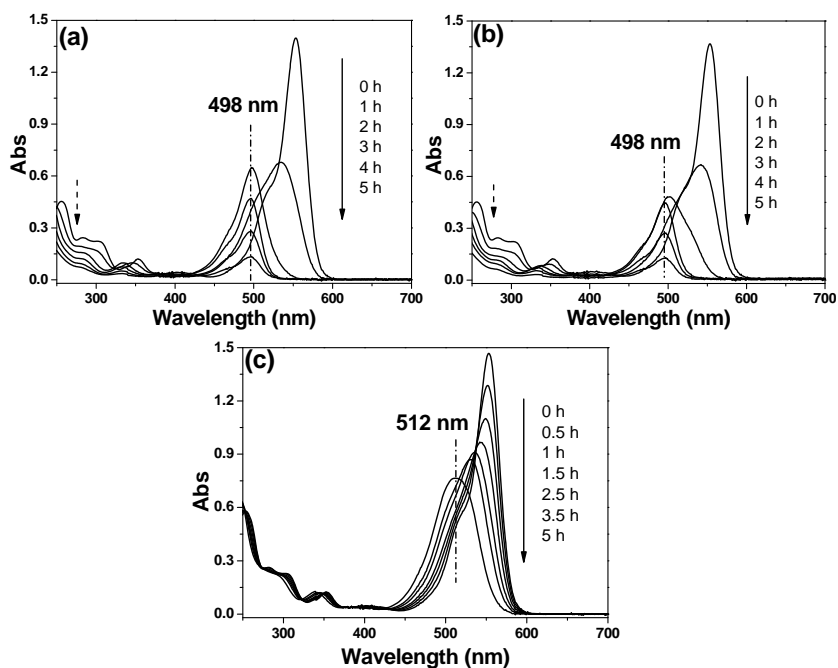


Fig. S8 Temporal UV-vis adsorption spectral changes for the RhB solution (20 μM) over TCHMs with (a) isopropanol, (b) methanol and (c) N_2 gas bubbling as a function of visible light irradiation time.

Isopropanol has been described as the best hydroxyl radical quencher due to its high-rate constant reaction with the radical, and widely used to discriminate the direct oxidation of substrates by holes or by $\cdot\text{OH}$ radicals.^{1,2} When isopropanol was added to the RhB solution in a concentration of 30 mM, however, negligible inhibition in RhB degradation was observed (Fig. S8a). This result suggests that the hydroxyl radical may play a minor role in this degradation process.

Moreover, in order to make clear whether or not the hole can be generated in $\text{TiO}_2@\text{C}$ under visible-light irradiation, methanol, which acts as an efficient holes scavenger^{3,4}, was added to the solution. As shown in Fig. S8b, in the presence of methanol as a hole scavenger, a fast photodegradation of RhB was occurred in the

reaction system, indicating the role of photogenerated hole in this system can also be negligible.

When the system was bubbled with N₂ gas to remove oxygen, the photocatalysis of TCHMs was extensively inhibited (Fig. S8c). Notably, only incomplete N-deethylation of RhB can be observed after 5 h visible light irradiation. This phenomena are similar to that observed in the RhB/THMs system, and the incomplete N-deethylation of RhB is attributed to the the self-photosensitized transformation of RhB over semiconductor. Based on the results, it is resonable to conclude that the superoxide radiacal ($\cdot\text{O}_2^-$), which is mainly dependent on the electron-transfer mediation, play a predominant part in the photo-oxidation of RhB over the TCHMs particles.

Moreover, the same experiments were also done by using TCMs as photocatalysts, and similar results can be obtained (data no shown).

Reference

1. R. Palominos, J. Freer, M. A. Mondaca and H. D. Mansilla, *J. Photochem. Photobiol., A*, 2008, **193**, 139-145.
2. A. Amine-Khodja, A. Boulkamh and C. Richard, *Appl. Catal., B*, 2005, **59**, 147–154.
3. T. Tachikawa, S. Tojo, K. Kawai, M. Endo, M. Fujistuka, T. Ohno, K. Nishijima, Z. Miyamoto and T. Majima, *J. Phys. Chem. B*, 2004, **108**, 19299–19306.
4. H. Petek and J. Zhao, *Chem. Rev.*, 2010, **110**, 7082-7099.